Abstract

Though the use of manganese bismuth in magneto-optical storage media has been previously studied, the prevailing method for growing MnBi films is unsuitable for read devices based on the spin polarized tunneling effect. Our coevaporation technique yields smoother and more homogenous films, which were analyzed for composition, topography, crystal structure, and magnetic properties. The films may be suitable for both magneto-optical recording and spin polarized tunneling in the same electrode. Marked improvements in storage capacity would result.

Introduction

The evolutionary trend of computers has encompassed marked improvement in speed and storage capacity, even while decreasing physical size. When existing limitations are reached, new technologies must be developed to meet the rising demands. Advances in storage capacity require the use of different materials and read-write techniques. Applications of both magneto-optical (MO) recording[1-3] and ferromagnet-insulator-ferromagnet (FM-I-FM) tunneling[4] are promising for improving storage capabilities.

Manganese bismuth (MnBi) is undergoing intense investigation[5-13] as a magneto-optical material. MnBi has a hexagonal NiAs crystal structure, with two equal axes separated by 120° and a third axis of different length, called the c-axis, perpendicular to both. MnBi has a very high magnetic anisotropy constant. The c-axis can be magnetized with a lower field than the other axes, and this is termed the direction of easy magnetization.[14] MnBi has a low optical density and an extremely large Kerr rotation, over 1° in the blue light wavelength range.[15] But because of its high spin polarization,[16] MnBi could also be used as an FM electrode in tunneling devices.[17]

Magneto-optical recording is predominantly used in current erasable optical disk drives. It utilizes a focused laser beam in the write process, locally heating a ferromagnetic thin film with perpendicularly oriented magnetization up to the Curie temperature T_c, at which its magnetic domains are completely randomized. During the cool down, the direction of magnetization of the material can be set by applying an appropriate magnetic field. In the read process, a focused beam of polarized light transmitting or reflecting from the magnetic thin film determines the magnetization direction of a "bit." The direction of magnetization dictates the beam's rotational direction of polarization, known as the Faraday or Kerr effect.[1] The larger the

Kerr rotation caused by a material, the smaller a magnetized "bit" needs to be to produce a differentiable signal. Therefore, a material's magneto-optical packing density is proportional to the magnitude of its Kerr rotation and reflectivity. This density is significantly greater than in films utilizing the inductive technique, in which a current is merely sent between two wire coils to set magnetization direction in the media.[2]

Another possible technology for increasing storage density is FM-I-FM read structures driven by the barrier tunneling phenomena.[4] Tunneling describes the movement of electrons across potential energy barriers, considered impossible by classical mechanics. However, Schrödinger's equation describes the behavior of quantum mechanical wave functions, whose probability densities indicate the position of electrons, within the potential energy barrier. As such waves exhibit exponential decay in this barrier, only a fraction of electrons actually cross the potential energy barrier, representing the insulator.[18] While tunneling can theoretically occur for any arbitrarily large energy barrier, the associated current is only measurable across ultra-thin (10–20 Å) insulating layers. In FM-I-FM structures, this current is dependent upon the metals' spin polarization, measuring the percentage of excess spin-up electrons in a material. As quantum theory maintains that spin is conserved, resistance is lower when spin-up electrons from the first FM layer tunnel to spin-up states, rather than spin-down states, in the second FM layer. Therefore, a resistance change occurs when the metal layer's relative direction of magnetization is changed. Resistance is low when magnetizations are aligned (greater density of spin-up states in both ferromagnets); resistance is high between antiparallel magnetizations.[17] The large difference in resistance, measured up to 32%,[19] allows for greater storage capacity, as smaller uniform regions could be employed as "bits."

Sequential evaporation methods are widely-used to prepare MnBi films for magneto-optical media. The process has developed as follows. Williams[6] first reported the preparation of ferromagnetic hexagonal MnBi films. Films were formed by vapor deposition of an Mn layer followed by a Bi layer on glass substrates. The bilayer was annealed at 250°C to 300°C for several days to form an alloy. The result was inhomogeneous MnBi, with the c-axis not perpendicular to the substrate plane. Chen[20] grew MnBi films by reversing the sequence of metal layers on mica substrates. The bottom Bi lattice grew with its c-axis oriented normal to the substrate plane. Mn atoms from the upper layer diffused downward to form epitaxial films, which exhibit crystals of one material growing in a definite orientation on the crystal face of another material. Others have slightly modified Chen's method with similar results: Nakada[21] optimized deposition conditions to reduce the required annealing temperature; Kido[22] utilized electron beam evaporation and ion beam annealing. However, these processes yield MnBi films with uncontrollable surface composition due to the possible incomplete atomic migration and surface oxidation. Therefore, while the sequential evaporation method is acceptable for magneto-optical media, it is unsuited for forming FM-I-FM tunnel structures, which require extremely clean FM surfaces.

Coevaporation of the elements should substantially increase compositional homogeneity in the films. Yoshida[23] examined films made by coevaporation of Mn and Bi, but these films did not yield the desired ferromagnetic phase.[24] In the present study, a new technique has been developed by which epitaxial ferromagnetic MnBi films have been grown successfully by the coevaporation method. Such films used as a top electrode in FM-I-FM structures could incorporate both magneto-optical recording and spin polarized tunneling. A laser focused on top would write the magnetization direction on this electrode, while tunneling resistance with the

bottom FM electrode would be detected by a read device. Storage capacity would increase from both an enhanced reading and writing technique.

Experimental

Thin films may be grown by several different *in situ* deposition techniques. Bulk materials may be sequentially evaporated to form layers on the substrate. An annealing process causes crystal formation. Materials may also be coevaporated to produce a uniformly mixed layer, and crystallization can be induced either by depositing materials onto a heated substrate or by annealing an amorphous film formed at low temperatures. Films may result in axis-oriented or epitaxial growth. Epitaxy occurs when an underlying seed layer provides an ordered lattice on which a film can grow. This seed coat may also serve as a nucleation layer, which increases nucleation sites as later discussed.

The MnBi films used in this study were prepared by coevaporation of the bulk metals in a vacuum of 10^{-7} to 10^{-8} torr.[I] Freshly cleaved mica, silicon wafers, and glass slides were used as substrates. Substrate temperature, monitored by a chromel-alumel thermocouple accurate to ±0.5°C, was maintained at 25°C to inhibit crystallization during deposition. Film thickness and deposition rate were regulated by a piezoelectric quartz monitor, which maintains accuracy to ±1Å. The materials were first deposited onto the substrate in the form of an ultra-thin Mn or Bi layer, Mn/Bi or Bi/Mn bilayer, or Mn/Bi/Mn trilayer. Metals were coevaporated at an atomic ratio of Mn_xBi_{1-x} (x = .500, .556, .600, .636, .667, .714) on top of this underlying coat. Films were annealed *in situ* from 2 to 24 hours at 300°C. A protective insulating layer of 20 to 250 Å thick Al_2O_3 was deposited over these films at liquid N_2 temperature (77K).

The most successful films used were prepared on glass according to the following procedure. A seed coat of bismuth, followed by manganese, was initially deposited at a 1:1

atomic ratio to form a 100 Å nucleation bilayer. The bulk metals of Mn and Bi were coevaporated (1:1 ratio) to form 1000 to 2000 Å films. The films were annealed 15 to 24 hours at 300°C. Finally, a 200 Å protective coat of Al_2O_3 was deposited over the MnBi film.

The composition of MnBi films was identified by scanning electron microscopy elemental analysis and Rutherford back scattering. Crystalline structure was determined by x-ray diffraction analysis (CuKα radiation). Film topography was examined by atomic force microscopy and scanning electron microscopy. The coercive field H_c and magnetic moment μ_B were determined by hysteresis-loop measurements at room temperature using a superconducting quantum interference device (SQUID). Films were tested with an applied magnetic field between -50 and 50 kOe.

Results and Discussion

It is known from earlier studies[25] that uniform magnetic MnBi films are not formed by a simple annealing process of bilayers. Instead, an underlying crystal layer must serve to nucleate and orient the MnBi to the desired crystal structure. The formation of MnBi starts at randomly distributed nucleation sites and continues radially around the starting point.[26] Because these nucleation sites are relatively rare,[25] a large portion of the Mn–Bi layer will not crystallize if growth is inhibited by irregularities on the substrate's surface. Therefore, it is necessary to control the number of nucleation sites to grow magnetic MnBi across the whole substrate. A bottom seed coat of Bi has also been shown[20] to induce the MnBi film's orientation. The Bi lattice provides a structure on which crystals grow with c-axis normal to the film plane. As previously mentioned, layers of various organization were used as the seed layer in this study:

Mn, Bi, Mn/Bi, Bi/Mn, and Mn/Bi/Mn. Only in films with a Bi/Mn nucleation bilayer are strong ferromagnetism and high c-axis orientation detected.

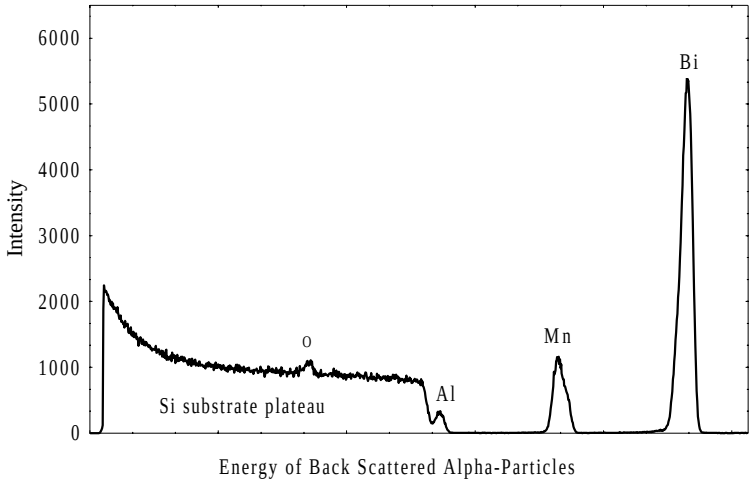

Figure 1. Rutherford back scattering data of MnBi films grown on Si substrate: 100 Å Bi/Mn nucleation layer, 500 Å coevaporated layer, 275 Å Al_2O_3 layer. Metals were evaporated at an atomic ratio 2:1. Resulting Mn to Bi atomic ratio is 2.38:1.

Previous work at the M.I.T. Francis Bitter Magnet Laboratory with ferromagnetic NiMnSb yielded high quality films when elements were deposited at a 1:1:1 atomic ratio.[27,28] A similarly simple process for MnBi was initially considered. However, past studies of MnBi films suggested a higher atomic Mn percentage for sequential evaporation to yield better quality MnBi films. Chen[9] used an initial atomic ratio ranging from 1.2:1 to 1.8:1, and the more recent studies by Rüdiger[26] reported a ratio of 1.9:1 to 2.5:1. These studies noted the loss of Mn due to an incomplete diffusion of Mn atoms, oxidation, or desorption.[10]

Our technique of coevaporation is shown by Rutherford back scattering[II] and scanning electron microscopy (SEM) elemental analysis[III] to result in a loss of Bi, specifically 16% (Fig. 1). The loss might be explained as Bi's 271°C melting point is lower than the film's 300°C annealing temperature. Such an annealing temperature is required to form MnBi in sequentially evaporated films, as the appearance of Mn_3O_4 in temperatures less than 300°C was reported.[26] Higher temperatures are not appropriate either, as they cause a change of Bi orientation and a lack of MnBi crystal structure. Thus, it can be asserted that crystal formation during

coevaporation must be performed at the same annealing temperature as during sequential evaporation.

Quality MnBi films can still be formed after a loss of material. Rüdiger[15] found that a final Mn percentage of 55–60% after annealing is needed to produce good films. As stated, sequentially evaporated films start at higher Mn ratios, losing Mn during the growth process. Our coevaporation method begins with an equal Mn to Bi ratio; Bi is lost during annealing. This Bi loss results in a desired Mn percentage (54%) in films prepared by our 1:1 method.

The MnBi films were structurally analyzed by x-ray diffraction (XRD).[IV] For films deposited at an atomic ratio 1:1, Figure 2 shows strong MnBi (002) and (004) and weak (008) peaks to be present, showing full texture with the c-axis oriented normal to the film plane. The lack of peaks due to other lattice planes and the intensity of (00*l*) peaks suggest epitaxial growth. Such growth is important in inducing perpendicular anisotropy, discussed later. Therefore, sequential and coevaporation methods yield MnBi films in the same crystalline form. Thin films prepared with higher Mn percentages show an abundance of peaks in the x-ray diffraction. Additionally, these films lack the dominant plane seen in Figure 2, suggesting that they are not as highly oriented.

Films were topographically examined using both SEM[III] and atomic force microscopy (AFM).[V] In 2000

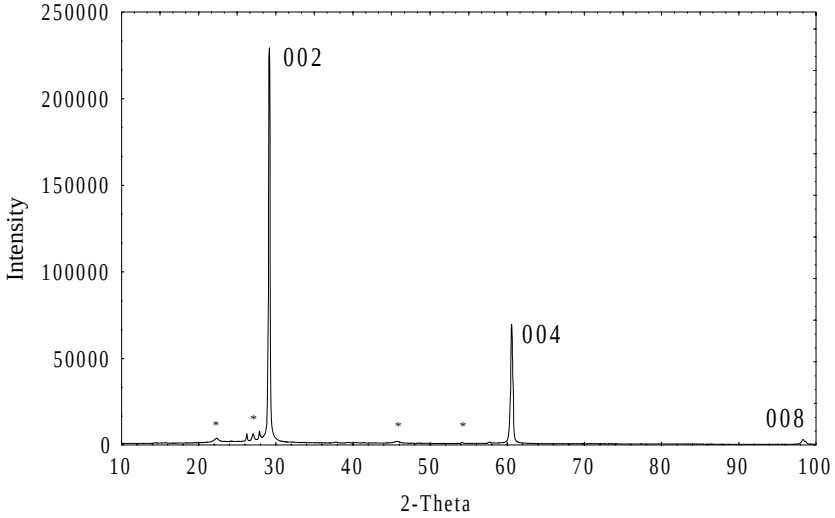

Figure 2. X-ray diffraction analysis of 1:1 atomic ratio 2000 Å MnBi films with 100 Å Bi/Mn nucleation layer and 200 Å Al_2O_3 layer. Annealed for 20 h at 300°C. MnBi peaks are marked with (00*l*) plane; * corresponds to a very small Bi

Å films prepared by the preferred 1:1 ratio method, general homogeneity (Fig. 3a) between distinct MnBi crystals is displayed. Both types of

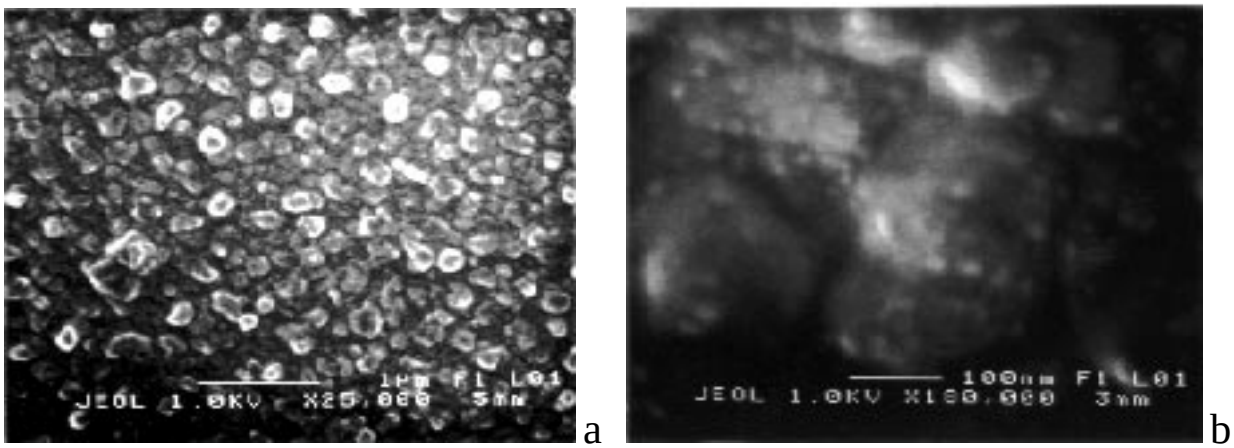

a b

Figure 3. SEM images of 1:1 atomic ratio 2000 Å coevaporated MnBi films with 100 Å Bi/Mn nucleation layer and 200 Å Al_2O_3 layer. Annealed for 15 h at 300°C.

microscopy show the mean grain size (mgs) of solitary crystals (Fig. 3b) to range from 100 to 400 nm. AFM (Fig. 4) calculates mean square roughness (Rq) to lie between 20 and 55 nm. AFM also relates the modeling of thin films in less than three dimensions, as height is extremely small compared to planar area. This technique, known as fractional dimensional analysis, measures a dimensionality between 2.39 and 2.99 in prepared MnBi films; the ideal thin film is two dimensional. The range of dimensionalities alludes to varying lm thicknesses across the substrate, supporting roughness measurements. A coalescence (Fig. 5) of underlying crystals is present in thicker films,

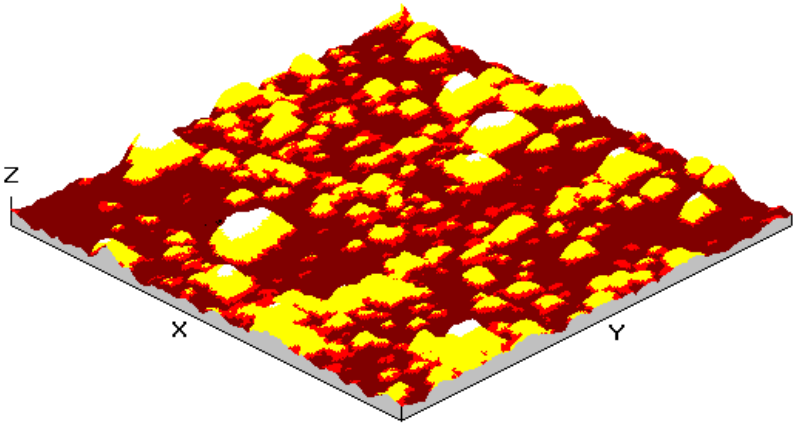

Figure 4. AFM image of 1:1 atomic ratio 2000 Å coevaporated MnBi films with 100 Å Bi/Mn nucleation layer and 200 Å Al_2O_3. Annealed for 20 h at 300°C. Dimensions of image: X = Y = 7.00 µm. Maximum height is 314.41 nm. Mgs = 400 nm, Rq = 53 nm, fractional dimensionality = 2.7046.

one of the factors increasing grain size and roughness. Preparing much thinner films can reduce this roughness significantly.

In films with higher Mn:Bi ratios, microscopy studies yield different results. SEM reveals bismuth crystallites on the surface, supporting the loss of Bi detected by compositional studies. AFM indicates a second Mn_xBi_{1-x} phase, comprised of much smaller crystals. For example, samples deposited at a 1.5:1 atomic ratio have a mgs of 70 to 90 nm and Rq of 5 to 8 nm. The presence of many phases in higher Mn-ratio films supports the XRD results previously discussed.

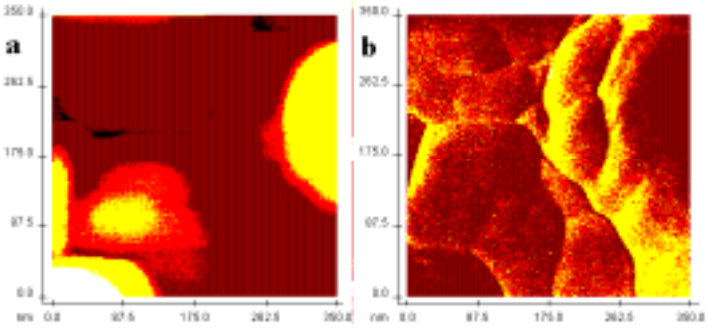

Figure 5. AFM magnification of MnBi film described in Fig. 4. Images were taken of the same regions, where (a) shows surface topography and (b) shows atomic force at each point. The variations of forces shown by (b) in what appear to be single crystals in (a) denote the coalescence of underlying crystals. Maximum height is 112.51 nm; maximum force is 22.47 nN. Mgs = 147 nm, Rq = 21.57 nm, fractional dimensionality = 2.7603.

SEM also shows the necessity for depositing *in situ* a relatively thick Al_2O_3 coat over the film. Corrosion was detected in films (Fig. 6) with a protective layer of <50Å. Films covered with a 200Å thick Al_2O_3 layer show no deterioration after several months. Such a coat does not impede tunneling devices, as internal junctions between FM electrodes do not experience atmospheric conditions.

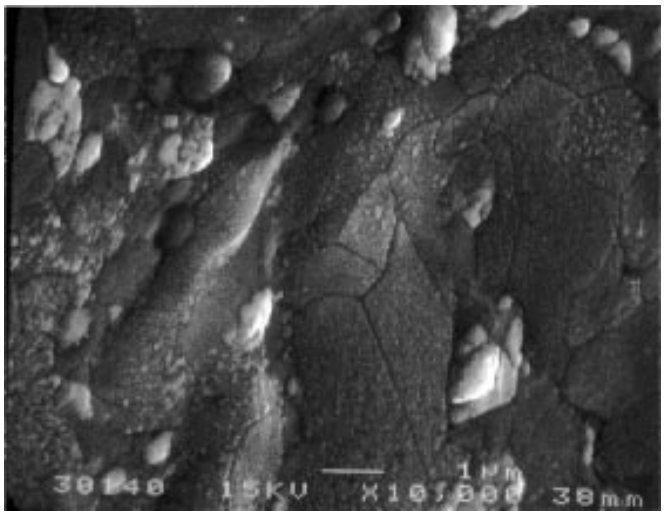

Figure 6. SEM image of 2:1 atomic ratio 500 Å coevaporated MnBi films with 100 Å Bi/Mn nucleation layer and 24 Å Al_2O_3 layer. Annealed for 20 h at 300°C. Corrosion is apparent in the film after exposure to atmospheric conditions for

The magnetic moment and coercive field of prepared MnBi films were determined by a superconducting quantum interference device (SQUID).[VIa] By detecting the magnetic flux variations in a substance due to applied field *H*, the magnetometer can determine the substance's magnetization *M*. This value of *M* must be taken into account when magnetization, or hysteresis, loops are examined with regard to the magnetization process in ferromagnets.[VIb] Figure 7 shows the hysteresis loop of MnBi when *H* is applied perpendicularly to the film plane at room temperature. *H* approaches the saturation point M_s (all magnetic domains are aligned) at 2.99×10^{-4} emu. From the saturation moment M_s, a magnetic moment per Mn atom of 0.58 μ_B is found.[VIc]

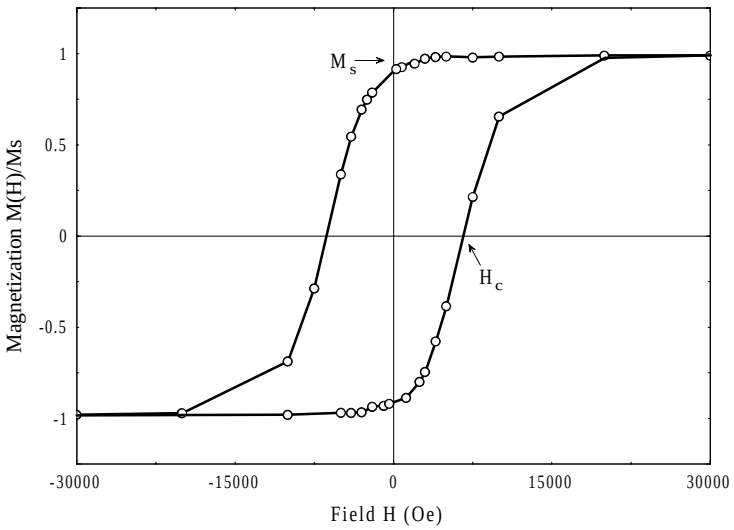

Figure 7. Hysteresis loop measured at 295K of 1:1 atomic ratio 2000 Å MnBi films with 100 Å Bi/Mn nucleation layer and 200 Å Al_2O_3 layer. Annealed for 20 h at 300°C. Field *H* applied perpendicular to sample.

When the applied field is reversed and *H* decreases to zero, *M* remains positive. Therefore, the prepared MnBi films are ferromagnetic by definition: magnetic dipole moments are permanently aligned. As the field increases in the negative direction, *M* becomes zero. The value of *H* at which this occurs, known as the coercive field H_c, describes the strength of coupled dipole moments to resist randomization. Surprisingly, the H_c of 6.4 kOe in coevaporated MnBi films is 10–20 times larger than data previously published.[7,9] To explain elevated H_c levels, domain theory has to be taken into account. Kittel[29] provides a detailed calculation of the coercive field:

$$H_c = H_{c,\infty}\left(1 - \frac{d}{d_o}\right)$$

where d is the crystal grain size, and $H_{c,\infty} = 2K/M_s$ is the maximum intrinsic coercive field, a function of anisotropy energy density K and saturation magnetization M_s. The length $d_o = 24\gamma/M_s$ is a function of domain wall energy γ and saturation magnetization.[26] Previous work[7,29,30] with sequentially evaporated films found particles of size d larger than 0.5 μm. As Figure 3b shows, films grown by the coevaporation method have isolated crystals with d values ranging from 0.1 to 0.4 μm. Therefore, due to the smaller d value, the coercive field H_c in coevaporated MnBi film is larger.

When the field H is applied parallel to the film plane, flux variations in the sample are not detected by the SQUID magnetometer. Even in external fields of 50 kOe, the magnetization of the sample is not noticeably induced. In other words, MnBi films resist magnetic moment alignment normal to the c-axis. Accordingly, coevaporated MnBi films have strong perpendicular magnetic anisotropy. In MO media, this anisotropy translates to clockwise or counterclockwise Kerr rotation during the reading phase, depending upon whether the direction of magnetization is up or down relative to the film plane.[1] As stated, MO storage density is a function of Kerr rotation and reflectivity.

Conclusions

MnBi films have been prepared *in situ* by coevaporation of the bulk metals. Material analysis was performed utilizing the techniques of Rutherford back scattering (composition), scanning electron microscopy (composition, topography), x-ray diffraction (structure), atomic force microscopy (topography on a finer scale), and SQUID measurements of the hysteresis loop. Films resulting from our preferred method (thin Bi/Mn nucleation layer and coevaporated layer at

1:1 atomic ratio) have single phase, epitaxial crystal structures. A loss of bismuth occurs during the annealing process. The MnBi films are ferromagnetic with a very high coercivity and strong perpendicular anisotropy.

Coevaporated MnBi prepared by our method has potential applications for both magneto-optical recording and FM-I-FM tunneling structures. The perpendicular anisotropy, epitaxial growth, and high coercivity of coevaporated are well suited for MO media. Decreased crystal size and improved surface homogeneity, compared to previous studies, make our method more suitable for MnBi's application as an FM electrode in surface-sensitive tunnel junctions. Coevaporation allows the growth of pure MnBi films more readily: the oxidation of manganese does not occur due to the lack of a surface Mn layer; the difficulty of verifying uniform and complete atomic diffusion in sequential deposition is not a factor. MnBi is currently being studied both doped or alloyed with other elements, including Sb,[31,32] Al,[33,34] Cu,[35] Ti,[36] and Si,[33] to improve its magneto-optical properties. Our coevaporation method could have similar advantages for such materials as it does for MnBi.

Acknowledgments

The author would like to thank J. Moodera for a position in his research lab at the M.I.T. Francis Bitter Magnet Laboratory. It is a pleasure to thank C. Tanaka for assistance with the evaporation equipment, x-ray diffraction, and SQUID measurements, and J. Nowak for AFM measurements. The author is indebted to those mentioned, P. LeClair, and D. Freedman for helpful discussions and suggestions. The research was partially funded through the NSF sponsorship of the residential Research Internship Program at Boston University.

Appendix

I. Deposition equipment and materials

Evaporation was performed *in situ* in a NRC 3116 Vacuum Coater, fitted with mechanical and diffusion pumps. It is capable of maintaining 1×10^{-8} torr pressures. The 99.99% pure manganese was produced by Johnson Mathey Materials Technology. Bismuth is 99.999% pure, fabricated by the United Mineral Chemical Corporation.

II. Rutherford Back Scattering

RBS is a technique used to test a material's elemental composition. The substance to be examined is bombarded by He nuclei (alpha particles), which are then scattered due to their repulsive Coulomb interaction with bare nuclei. The angular distributions of scattered α-particles allude to a heavy charged center in the scattering material that has a charge proportional to its atomic number. While Rutherford's experiment led to the first model of a nuclear atom, it also provided a method of compositional analysis. As the scattering angle is a function of the target's nuclear charge and the mass, charge, and velocity of the bombarding particle, one can determine the material's composition by the distribution. RBS was performed at Harvard University's Gordon McKay Laboratories. Films analyzed by this method were deposited on silicon to minimize background noise caused by the complex elemental structures of the mica and glass substrates.

III. Scanning Electron Microscopy

SEM is a method to determine a material's topography and composition. A beam of electrons is focused by a succession of precisely placed cylindrical electrodes. The beam scans

the surface of a sample, causing secondary electrons to be emitted by the material. The distributions of secondary electrons are used to create a visual image. To determine chemical composition, a monitor detects x-rays coming from the sample. Each element has different interband transitions. Based on the location and intensity of the peak in the spectrum, the chemical composition can be determined. A Joel JSM Scanning Microscope was used at Harvard's Gordon McKay Lab for enlargements up to 10,000× and at M.I.T.'s Department of Materials Science and Engineering for magnifications up to 300,000×.

IV. X-Ray Diffraction

XRD is a means to determine a solid's crystalline structure. In any crystal, many sets of parallel planes (Bragg planes) can be drawn to pass through atomic positions, and a characteristic distance (Bragg spacings) exists between planes. For each Bragg plane, x-rays in principal reflect at a given incident angle equal to the reflection angle. If the distance between planes is d, the difference in path lengths of rays is $2d\sin\theta$ (where θ is the angle between the x-rays and the Bragg plane). When this difference is an integer multiple of the x-ray wavelength, constructive interference occurs between reflected rays, and a peak in intensity is observed at that θ value. This is known as Bragg's law:

$$2d\sin\theta = n\lambda \qquad \text{where } n = 1, 2, 3...$$

As Bragg spacings (d) are equal, constructive interference occurs between all rays scattered from the crystalline planes at a limited set of θ. While θ measures the angle between the reflected beam and the surface plane, it is much more convenient experimentally to measure the angle between the reflected and transmitted beam, which is 2θ. The 2θ values can thus be calculated:

$$2\theta = 2\sin^{-1}\left(\frac{\lambda}{2d}\right)$$

XRD was performed at M.I.T.'s Center for Materials Science and Engineering, using a Rigaku Rotaflex RU 300. CuKα radiation (λ = 1.5418 Å) was used for scattering at 300 mA and 60 kV. The *d* values of MnBi are not present in the Powder Diffraction Files. So, x-ray diffraction patterns were simulated by the computer application Powder Cell 1.8 (W. Kraus and G. Nolze, BAM 12489, Berlin), which calculated *d* spacings at $10° < 2\theta < 70°$. The peak observed at 98.3° was identified as MnBi (008) due to its intensity and 2θ value. When one peak is present representing a lattice plane (002), then other parallel planes should be present, which are integer multiples (004), (008). The MnBi unit cell parameters[38] used for this simulation are as follows:

System: hexagonal	Mn_1 position: 0.000 0.000 0.000
Space group: $P6_3/mmc$	Mn_2 position: 0.000 0.000 0.500
Unit cell dimensions: [39]	Bi_1 position: 0.333 0.667 0.250
a = 4.287Å, b = 4.287Å, c = 6.118Å	Bi_2 position: 0.667 0.333 0.750

V. Atomic Force Microscopy

AFM is a method to study topography of both conducting and nonconducting surfaces. A small cantilever held close to the sample scans across the surface, changing in height depending upon the local atomic forces. As "peaks" or "valleys" in the film are scanned, the atomic force repulsion causes the cantilever to rise or fall. A constant distance between surface and tip is maintained by a piezoelectric monitor, holding a constant force between tip and substrate. Microscopy was performed using a Burleigh Metris 2000 AFM at the Francis Bitter Magnet Lab.

VI. Superconducting Quantum Interference Device

A. The SQUID magnetometer is used to measure very small magnetic fluxes in a substance. These flux variations are detected by placing the sample between two parallel superconductors, separated by a thin insulating strip. The tunneling structure, known as a Josephson junction, forms a single quantum system: pairs of electrons as a unit, rather than individual electrons, tunnel through the barrier. One consequence is that even in the absence of a potential difference between two identical superconductors, a tunneling current will flow across a Josephson junction. This is called the DC Josephson Effect.[40]

The two junctions in parallel cause an interference pattern to appear in the net current. The pattern is affected by a magnetic flux enclosed by the two arms of the pair of junctions. The dependence of the current on the enclosed magnetic flux Φ_B is given by the equation:

$$J = J_{max} \cos\left(\frac{e\Phi_B}{\hbar}\right)$$

where e is the charge of an electron, and $\hbar = h/2\pi$, h being Planck's constant. SQUID measurements were performed with a Quantum Design AC / DC MPMS-5S at M.I.T.'s Center for Materials Science and Engineering.

B. When the SQUID is used to generate M-H loops, the magnetization of the substrate must be taken into account:

$$M_{total} = M_{MnBi} + M_{substrate}$$

The magnetization of the substrate is equal to χH_{total}, where χ is the susceptibility of the substrate. In a ferromagnetic material, even as H increases without bound, M asymptotically approaches its constant saturated value of M_s, which signifies the alignment of all magnetic domains. However, the experimentally measured M-H loop shows a constant decrease after the saturation magnetization M_s has been reached. Thus, the decrease demonstrates that the

magnetometer detects the diamagnetic glass substrate, which intrinsically has no permanent magnetic dipole moments. As the field increases, so does the flux through an electron's orbit. According to Lenz's law, the electron in a diamagnetic material will counter the changing flux by increasing angular momentum and orbital magnetic moment (in the negative direction).[41] Therefore, the susceptibility χ has a negative value, resulting in a smaller observed M_{total} for the sample, since $M_{substrate}$ is negative.

C. As all the magnetic moments in a ferromagnetic material are aligned at saturation, magnetization can be expressed in terms of the Bohr magnetons μ_B per Mn atom. The Bohr magneton (9.27402×10^{-21} emu) is a measure of the magnetic moment of one electron:

$$\mu_B = \frac{e}{2m_e}\hbar$$

where e is the electron's charge, m_e is the electron's mass, and $\hbar = h/2\pi$.

Bibliography

1. M. Kryder, MRS Bulletin 21, 17 (1996).
2. J. Brug, T. Anthony, and J. Nickel, MRS Bulletin 21, 23 (1996).
3. T. Suzuki, MRS Bulletin 21, 42 (1996).
4. J.S. Moodera and L.R. Kinder, J. Appl. Phys. 79, 4724 (1996).
5. B.W. Roberts, Phys. Rev. 104, 607 (1956).
6. H.J. Williams, R.C. Sherwoord, F.G. Foster, and E.M. Kelley, J. Appl. Phys. 28, 1181 (1957).
7. D. Chen, J.F. Reach, and E. Bernal, J. Appl. Phys. 39, 3916 (1968).
8. W.K. Unger and M. Stolz, J. Appl. Phys. 42, 1085 (1971).
9. D. Chen, J. Appl. Phys. 37, 1486 (1966).
10. D. Chen, G.N. Otto, and F.M. Schmitt, IEEE Trans. Magn. 66 (1973).
11. R. Atkinson, Thin Solid Films 37, 195 (1976).
12. M.A. Angadi and V. Thanigaimani, J. Mat. Sci. Let. 6, 1004 (1987).
13. X. Guo, X. Chen, Z. Altounian, and J.O. Shtron-Olsen, J. Appl. Phys. 73, 6275 (1993).
14. C. Guillaud, thesis, University of Strasbourg (1943).
15. S. Uchiyama, J. Magn. Soc. Japan 17, (suppl 1) 1 (1993).
16. W. Zuowoi and H. Meichun, Chinese Phys. Let. 10, 612 (1993).
17. R. Meservey and P.M. Tedrow, Phys. Rep. 238, 174 (1994).
18. A.P. French and E. Taylor. *An Introduction to Quantum Physics.* (Norton and Co., New York, 1978).
19. J.S. Moodera, L. Kinder, T. Wong, and R. Meservey, Phys. Rev. Let. 74, 3273 (1995).
20. D. Chen, J. Appl. Phys. 42, 3625 (1971).

21. M. Nakada and M. Okada, IEEE Trans. Magn. 30, 4431 (1994).

22. Y. Kido and M. Suzuki, Mat. Let. 7, 219 (1988).

23. K. Yoshida, K. Dejima, M Nishijima, and T. Yamada, J. Crystal Growth 45, 376 (1978).

24. K. Yoshida and T. Yamada, Appl. Surface Science 33-4 (1988).

25. L. Mayer, J. Appl. Phy. 31, 384S (1960).

26. U. Rüdiger, H. Berndt, A. Schirmeisen, P.Fumagalli, and G. Güntherodt, J. Appl. Phys. 78, 5391 (1995).

27. R. Kabani, M. Terada, A. Roshko, and J.S. Moodera, J. Appl. Phys. 67, 4898 (1990).

28. J.S. Moodera and D.M. Mooto, J. Appl. Phys. 76, 6101 (1994).

29. C. Kittel, Phys. Rev. 73, 810 (1948).

30. D. Chen, J. Appl. Phys. 38, 1309 (1967).

31. A. Andresen, J. Engebretsen, and J. Refsnes, ACTA Chem. Scan. 26, 175 (1972).

32. Z. Celinski, D. Pardo, B. Engel, and C. Falco, IEEE Trans. Magn. 31, 3233 (1995).

33. J. Shen, R. Kirby, and D. Sellmyer, J. Magn. Magn. Mat. 81, 107 (1989).

34. Y.J.Wang, J. Magn. Magn. Mat. 84, 39 (1990).

35. J. Shen, K. Wierman, R. Kirby, and D. Sellmyer, IEEE Trans. Magn. 31, 3334 (1995).

36. H. Göbel, E. Wolfgang, H. Harms, Phys. Stat. Sol. 34, 553 (1976).

37. B.D. Cullity, *Elements of X-Ray Diffraction* (Addison Wesley, Reading, MA, 1978).

38. R. Wyckoff, *Crystal Structures*, Vol 1 (John Wiley & Sons, 1963).

39. C. Guillaud, J. Phys. (Paris) 12, 239 (1951).

40. P. Fishbane, S. Gasiorowicz, and S. Thornton, *Physics for Scientists and Engineers* (Prentice Hall, Englewoof Cliffs, NJ).

41. E. Purcell, *Electricity and Magnetism* (McGraw Hill, New York, 1985).